Paracrine FGF1 signaling directs pituitary architecture and size

Konstantin Khetchoumian, Kevin Sochodolsky, Chrystel Lafont, Arthur Gouhier, Amandine Bemmo, Yacine Kherdjemil, Marie Kmita, Paul Le Tissier, Patrice Mollard, Helen Christian, et al.

Paracrine FGF1 signaling directs pituitary architecture and size

Running Title: Interactions between corticotropes and somatotropes

Konstantin Khetchoumian[1]*, Kevin Sochodolsky[1], Chrystel Lafont[2,3], Arthur Gouhier[1], Amandine Bemmo[1], Yacine Kherdjemil[4], Marie Kmita[5], Paul Le Tissier[6], Patrice Mollard[2,3], Helen Christian[7], Jacques Drouin[1]*

[1]Laboratoire de génétique moléculaire, Institut de recherches cliniques de Montréal (IRCM)
Montréal QC, H2W 1R7 Canada
[2]Institute of Functional Genomics, University of Montpellier, CNRS, INSERM, F-34094 Montpellier, France
[3]BioCampus Montpellier, University of Montpellier, CNRS, INSERM, F-34094 Montpellier, France
[4]IRCM Disease Modeling and Genome Editing platform
[5]Laboratoire de recherche en génétique et développement, (IRCM)
[6]Centre for Integrative Physiology
University of Edinburgh
Edinburgh UK
[7]Oxford University, Department of Physiology, Anatomy & Genetics - Le Gros Clark
South Parks Road Science area Le Gros Clark Building
South Parks Road
Oxford OX1 3QX, UK

Keywords: Cell-cell interactions, FGF1, organogenesis, cell networks, GH deficit, secretion

***Corresponding authors and to whom address reprint request:**

Jacques Drouin and Konstantin Khetchoumian
Laboratoire de génétique moléculaire
Institut de recherches cliniques de Montréal (IRCM)
110 Avenue des Pins Ouest
Montréal QC H2W 1R7 Canada
Tel.: (514) 987-5680; Fax: (514) 987-5575
jacques.drouin@ircm.qc.ca
Konstantin.Khetchoumian@ircm.qc.ca

This work was supported by grants from the Canadian Institutes for Health Research (CIHR) to JD.

ABSTRACT.

Organ architecture is established during development through intricate cell-cell communication mechanisms, yet the specific signals mediating these communications often remain elusive. Here we used the anterior pituitary gland that harbors different interdigitated hormone-secreting homotypic cell networks to dissect cell-cell communication mechanisms operating during late development. We show that blocking differentiation of corticotrope cells leads to pituitary hypoplasia with a major effect on somatotrope cells that directly contact corticotropes. Gene knockout of the corticotrope-restricted transcription factor Tpit results in fewer somatotropes, with less secretory granules and a loss of cell polarity, resulting in systemic growth retardation. Single cell transcriptomic analyses identified *FGF1* as a corticotrope-specific *Tpit* dosage-dependent target gene responsible for these phenotypes. Consistently, genetic ablation of *FGF1* in mice phenocopies pituitary hypoplasia and growth impairment observed in *Tpit*-deficient mice. These findings reveal FGF1 produced by the corticotrope cell network as an essential paracrine signalling molecule participating in pituitary architecture and size.

SIGNIFICANCE.

The development of complex organs relies on cell-cell interactions that are precisely orchestrated during organogenesis. Although it appears as a random patchwork of hormone-producing cells, the pituitary gland is constituted of homotypic cell networks in which cells of the same lineage maintain contacts that are crucial for function. There are also privileged heterotypic interactions but of unknown significance. Here, we investigated how the loss of cell identity in one cell lineage impacts function of another lineage. Using single cell transcriptomics, we thus identified FGF1 expressed in corticotrope cells as an important signal for somatotrope cell identity and function. The present work uncovers a pituitary role of FGF1 that was discovered in pituitary extracts, but without a known function until now.

The pituitary gland is a crucial component of the neuroendocrine system regulating vital body functions such as homeostasis, metabolism, reproduction, growth, response to stress and lactation. Present in all vertebrates, it is also referred to as the body's “master gland” because it controls the activity of most other hormone-secreting glands. The development of the anterior pituitary (AP) involves a coordinated spatial and temporal sequence of events that ultimately gives rise to five pituitary endocrine cell populations (corticotropes, gonadotropes, lactotropes, somatotropes and thyrotropes) (1), together with support cells, pituitary stem cells (PSC) (2-5) and a vascular network of endothelial cells wrapped by pericytes (6). The endocrine (glandular) part of the pituitary derives at embryonic day 9.5 (e9.5 in mice) from a midline invagination of the oral ectoderm called Rathke’s pouch (1, 7). Different endocrine cell types are sequentially specified and differentiate from this epithelium starting in mice with corticotropes (e12.5) (8), followed by the Pit1/Pou1f1-dependent lineages (9, 10) – thyrotropes (e14.5), somatotropes (e15.5), lactotropes (e16,5) - and by gonadotropes (e17.5) (11). Differentiation occurs in parallel with tissue expansion and this process continues during the first weeks after birth (12-14). Whereas postnatal pituitary development is less investigated, embryonic pituitary development is relatively well characterized, with many signaling pathways and transcription factors involved in early (including BMP2/4/7, FGF8/10/18, Wnt4/5a, Lhx3/4, Pitx1/2 and Prop1) or late (Tpit, Pax7, Pit1/Pou1f1, SF1/NR5A1, GATA2, NeuroD4) steps of fetal development (1, 7, 15). The demand for hormone secretion rises after birth, and this is met by ≈10-fold organ growth during the first four weeks after birth (13, 16). Both cell size (17) and number (12-14, 16, 18, 19) are increased during this period, in parallel with a ≈100-fold

increase of hormone gene transcription (19, 20). Bulk proliferation in the late postnatal pituitary (>2-weeks) comes from Sox2-negative/hormone-negative committed progenitors. A recent study elegantly showed that this expansion depends on WNT signaling provided by Sox2-positive PSC (21), and suggested other secreted factors, such as FGFs, may regulate expansion of progenitors by several paracrine mechanisms. Interestingly, the founding members of the FGF family, FGF1 and its closest paralog FGF2, were originally identified in pituitary extracts (22, 23) as factors stimulating fibroblast proliferation (24, 25). However, no *FGF1/2* function was described in pituitary so far. *FGF1* inactivation in mice didn't reveal any notable phenotype in standard laboratory conditions and didn't affect the mild phenotype of *FGF2* knockout mice (26). More recently, FGF1 was shown to play an important role in maintaining metabolic homeostasis in adipose tissue in response to fluctuations in nutrient availability (27). Transcriptomic analysis of sorted pituitary Sox2-positive PSCs showed enrichment for transcripts encoding FGF signaling pathway components (21). However, the expression and source of FGFs in specific pituitary cells has not been investigated.

Recent seminal studies showed that different pituitary cell populations are organized in homotypic networks (28-32). While the discovery of pituitary cell networks profoundly changed our view on how this organ is organized and functions, it opened novel questions, namely: are different cell networks communicating with each other, and if yes - how? Indeed, preferential contacts between pituitary cells of different lineages were observed, for example between corticotropes and somatotropes (33, 34) and between corticotropes and gonadotropes (29, 31). These observations suggest preferential heterotypic communication between developmentally distinct lineages, for example for

the corticotrope and somatotrope networks. To test this hypothesis, we took advantage in the present work of mutant mice deficient for the corticotrope differentiation transcription factor Tpit (*Tpit*-KO mice) (35). The *Tpit*-deficient AP appears normal by the end of embryogenesis, but becomes hypoplastic starting around 3 weeks of age, with a particular effect on somatotropes and resulting in growth retardation. Single cell transcriptomics revealed *FGF1* as a corticotrope-specific Tpit target gene downregulated in *Tpit* mutant mice. Further, mice inactivated for *FGF1* phenocopy the phenotypes observed in *Tpit*-KO mice, revealing a paracrine cell communication (corticotrope-somatotrope) mechanism coordinating postnatal pituitary organogenesis.

Results

A smaller anterior pituitary in *Tpit*$^{-/-}$ mice. Within the AP, Tpit is only expressed in corticotropes that represent <10% of cells (1, 29, 36). The *Tpit* mutation is thus not expected to significantly affect pituitary size. However, adult *Tpit*$^{-/-}$ (*Tpit*-KO) pituitaries are smaller than wild-type (WT) sibling controls (Fig. 1*A* and *SI Appendix* S1*A*). To quantify the cell number contribution to this difference, we measured DNA contents in adult (3-4 months) pituitaries of WT, *Tpit*$^{+/-}$ (*Tpit*-HT) and *Tpit*-KO mice of both sexes. Surprisingly, the AP is smaller not only in *Tpit*-KO, but also in *Tpit*-HT animals, with a stronger phenotype in females (Fig. 1*B*). Because *Tpit*-KO mice fail to produce ACTH and are in adrenal insufficiency, the reduced pituitary size could be secondary to glucocorticoid (Gc) deficiency or to other endocrine interactions. However, this is unlikely because neither heterozygous mice (37) nor human heterozygous carriers of mutated *TPIT* alleles show Gc deficiency (38, 39). But to leave no doubt, we assessed

pituitary size in *POMC*-KO mice (40), a model that exhibits a similar ACTH deficiency compared to the *Tpit*$^{-/-}$ model. In contrast to *Tpit*-KO pituitaries, *POMC*$^{-/-}$ pituitaries have a similar size compared to controls (Fig. 1*B* and *SI Appendix* S1*B*). Therefore, the AP cell number correlates with *Tpit* gene dosage.

We next determined when AP hypoplasia appears in *Tpit*-KO and HT mice. Tpit expression starts at the embryonic day e12 (1) and at e18.5, the size of *Tpit*-KO and HT pituitaries appeared normal (*SI Appendix* Fig. S1 *C* and *D*), indicating AP hypoplasia develops postnatally. We included HT mice to determine direct roles of Tpit on postnatal pituitary development as opposed to consequences of Gc deficiency caused by the absence of Tpit. Similar to previous reports (21), we observed two postnatal phases of pituitary growth (Fig. 1 *C* and *D*). Tpit deficient mice were born with pituitaries of normal size and did not show any delay in the first (rapid) phase of postnatal growth (3-weeks) before weaning. However, both *Tpit*-HT and KO show pituitary growth retardation at the second (slow) phase of growth (P22-P≥90). Evaluation of pituitary cell proliferation by Ki67 labeling revealed reduced proliferation rates in *Tpit*-HT animals of both sexes at 3-weeks, but this was not the case at P5 (Fig. 1 *E* and *F*). In summary, Tpit, expressed in ≈10% pituitary cells (corticotropes), regulates in a dosage-dependent manner the overall pituitary size during the second phase of postnatal growth (proliferation) starting at 3 weeks of age.

GH deficiency in *Tpit*$^{-/-}$ mice. Previous reports suggested preferential contacts between corticotropes and somatotropes based on immunolabeling on pituitary sections (33, 34). Using 2-photon microscopy on thick pituitary slices, we confirmed that ACTH-

positive corticotropes have frequent intimate contacts with GH cells with the cytoplasm of corticotropes often surrounding GH cells (Fig. 2*A*). Since homotypic interactions between GH cells were shown to involve adherens junctions revealed by presence of β-Catenin at these junctions (41), we performed co-labeling for GH and β-Catenin on sections of e18.5 POMC-eGFP mouse pituitaries (20). Strong β-catenin signals were indeed observed at contacts between GH cells (Fig. 2*B*), but also at contacts between GH and POMC cells (Fig. 2*C*). In contrast, homotypic contacts between POMC cells do not present such strong β-Catenin signal, although weak β-Catenin may also be present at these contact points (Fig. 2*D*). Surfacing and quantification revealed an important (>80%) colocalization between β-Catenin/POMC and GH signals (Fig. 2*E* and *F*). These observations led us to analyze in detail the activity of GH cells in *Tpit*-KO mice that fail to differentiate corticotropes (8, 35). We first assessed the expression of pituitary GH mRNA by RT-qPCR. Strikingly, GH mRNA levels are decreased by about 50% in *Tpit*-KO males and by 70% in females (Fig. 2*G*). We also confirmed the loss of POMC expression in *Tpit*-KO pituitaries and showed that *Tpit*-HT pituitaries have normal levels of POMC mRNA (Fig. 2*G*) as previously noted (37).

We measured pituitary GH contents to correlate the decreases in GH mRNA with hormone synthesis. Decreased GH contents were observed in both male and female *Tpit*-KO pituitaries (Fig. 2*H*), with dosage sensitivity in males (32% reduction in HT and 58% reduction in KO), and a similar tendency in females with a more dramatic effect in KO (84% reduction) in agreement with mRNA levels.

Liver IGF1 mRNA provides a measure of effective circulating GH. We found decreased IGF1 mRNA levels in KO livers in both sexes (Fig. 2*I*), with a greater *Tpit* dosage

dependency and a stronger decrease in females, correlating with the greater loss of GH contents (Fig. 2 *G* and *H*).

We then determined when GH deficiency develops in *Tpit*-KO and HT animals. GH staining did not reveal any difference in e18.5 *Tpit*-HT and KO pituitaries (*SI Appendix* Fig. S2 *A*-*D*). In contrast, the proportion of GH-positive cells is reduced in *Tpit*-HT mice of both sexes at 3-weeks after birth (Fig. 2*J*-*K*). In agreement with this, *Tpit*-KO mice are growth-retarded (Fig. 2*L*-*M* and *SI Appendix* Fig. S2 *E*-*G*).

Altogether, the data suggest that functional interactions between corticotropes and somatotropes occur postnatally and that the loss of *Tpit* (which is only expressed in POMC cells) results in pituitary GH deficiency with resulting systemic manifestations.

Ultrastructural abnormalities and loss of secretory granule polarity in GH cells of *Tpit*$^{-/-}$ pituitaries. We then used electron microscopy to assess whether somatotrope cell structure is altered in *Tpit*-KO pituitaries. The basic somatotrope ultrastructural organization is preserved (Fig. 3 *A*-*I*) and specific GH immunogold labeling revealed secretory granules in all three *Tpit* genotypes. However, both *Tpit*-HT and *Tpit*-KO pituitaries appear to have less GH granulation than WT. The polarity of secretory granules (accumulation of granules in the direction of capillaries) is an indication of coordination between hormone-secreting cells and the microvasculature necessary for secretory activity. Compared to normal (WT), *Tpit*-HT and *Tpit*-KO somatotropes displayed less polarity of secretory granules towards capillaries, with the null phenotype being more severe (Fig. 3*D*, 3*E*, 3*G*, 3*H*). Around 20% of KO somatotropes showed

increased granule margination (Fig. 3*I*). A smaller number of HT somatotropes also showed margination (Fig. 3*F*). No differences in RER expansion could be observed.

In *Tpit*-HT and KO mice, somatotrope areas (Fig. 3*J*) were significantly reduced ($P < 0.05$) compared with WT, as were granule areas (Fig. 3*K*) and granule diameters (Fig. 3*L*, $P < 0.01$). Therefore, the smaller appearance of *Tpit* mutant pituitaries reflects both reduced cell number (hypoplasia) and somatotrope cell size.

In summary, *Tpit* inactivation affects somatotrope size and their ability to accumulate secretory granules on the apical/capillary side of the cell. These effects are gene dosage-dependent. Cell size and granule polarity changes suggest disturbances at the level of the cytoskeleton and/or protein transport in somatotropes. The underlying reason is not obvious, as these alterations in somatotrope cell ultrastructure are caused by inactivation of a regulator of corticotrope cell identity that is only expressed in corticotropes. The margination of secretory granules together with their decrease in number and size is likely reducing the efficiency of GH response to secretagogues, further contributing to GH deficiency in *Tpit*-KO mice.

***Tpit* haploinsufficiency causes transcriptomic changes in Tpit-positive and Tpit-negative pituitary cells.** We performed single-cell RNA-sequencing (scRNAseq) on 3-month-old male pituitaries (two per sample) from WT, *Tpit*-HT and *Tpit*-KO mice in order to assess transcriptomic changes caused by *Tpit* deficiency in the different pituitary lineages. A total of 37,474 WT (11,222), *Tpit*-HT (12,839) and *Tpit*-KO (13,413) cells were assayed. Cell clusters identified by Uniform Manifold Approximation and Projection (UMAP) (42) were annotated based on the expression of key pituitary marker genes (*SI*

196 *Appendix* Fig. S3 *A* and *B*). While 21 similar clusters were identified in WT and HT
197 samples, KO samples lack the two POMC clusters (corticotropes and melanotropes), in
198 agreement with the essential role of *Tpit* for pituitary POMC expression (35) and POMC
199 cell terminal differentiation (17) (Fig. 4*A* and 4*B*). Instead, *Tpit*-KO pituitaries contain
200 more cortico/gonado-trope precursors and gonadotropes (Fig. 4 *A* and *B* and *SI*
201 *Appendix* Fig. S3 *A* and *B*), confirming previous reports suggesting the existence of
202 common cortico/gonado-trope precursors and showing an antagonism between
203 corticotrope and gonadotrope fates (29, 35). Strikingly, the absence of Tpit also led to
204 important perturbations in two somatotrope clusters: cluster #1 shifted position, while
205 cluster #2 disappeared and a novel cluster (#5) appeared instead (Fig. 4*A*). Overall,
206 total somatotrope percentage decreased proportionally to *Tpit* dosage (Fig. 4*B*). We
207 then performed differentially expressed gene (DEG) analysis to identify *Tpit*-dependent
208 genes. In agreement with changes observed in cluster analyzes, the absence of *Tpit*
209 mostly led to transcriptomic perturbations in cortico/gonado-trope precursors,
210 gonadotropes and somatotropes (*SI Appendix* Fig. S3*C*). Since the absence of Tpit
211 leads to POMC and consequently Gc deficiencies, we cannot attribute with certitude
212 gene expression differences observed in *Tpit*-KO animals directly to Tpit. Therefore, we
213 focused our analyzes on HT mice that do not show any Gc deficiency (37).As expected,
214 the biggest changes are observed in Tpit-positive cells, namely corticotropes and
215 melanotropes (Fig. 4*C*). In corticotropes, more than half (41/68) of genes downregulated
216 in *Tpit*-HT mice (*SI* Dataset 1) correspond to corticotrope signature genes (Fig. 4*D*), as
217 identified by Seurat analyzes (*SI* Dataset 2), supporting the important role of Tpit in
218 corticotrope identity. Interestingly, several genes encoding secreted or plasma

membrane proteins are deregulated in *Tpit*-HT corticotropes (Fig. 4*D*). The second most affected population in *Tpit*-HT pituitaries are somatotropes (mainly cluster #2: Fig. 4*C*), suggesting an important signaling from corticotropes to somatotropes. Transcriptomic comparison of WT *vs* HT cluster #2 somatotropes identified 105 DEGs (Fig. 4*E* and *SI* Dataset 3). The most significantly enriched biological processes associated with these genes identified by gene ontology (GO) analysis are in the MAPK/Ras and PI3K signaling pathways (Fig. 4*F*). In particular, several positive regulators of the MAPK pathway are upregulated (*Hspa1a, Hspa1b, Igf1, Trim5*) while a negative regulator (*Efna1*) is downregulated (Fig. 4*G*), suggesting an activation of the MAPK pathway. This may reflect compensatory feedback to the reduction of GH signaling, or decreased signaling from corticotropes (e.g. *FGF1, Wnt4, Wnt9a*: see Fig. 4*D*). All these deregulations are also present in *Tpit*-KO somatotropes and in most cases, they are *Tpit* dosage sensitive (Fig. 4*G*), suggesting they are direct consequences of Tpit-dependent deregulations in corticotropes. Complete *Tpit* inactivation resulted in much more dramatic changes in somatotropes, leading to major transcriptome changes in cluster #5 compared to cluster #2, with 781 deregulated genes (*SI Appendix* Fig. S4*A*, S4*B* and Dataset 4).

This may reflect corticotrope-dependent and systemic (i.e. Gc deficiency) consequences of Tpit absence. GO analyzes also revealed perturbations of proliferative pathways in *Tpit*-KO somatotropes (*SI Appendix* Fig. S4*C*).

In summary, *Tpit* haploinsufficiency leads to transcriptomic changes in both Tpit-positive and Tpit-negative pituitary cells, suggesting a communication between these cell types, namely between corticotropes and somatotropes.

***Tpit* gene dosage-dependent FGF1 expression for corticotrope-somatotrope crosstalk.** To identify Tpit-dependent genes involved in cell-cell interactions, we used CellPhoneDB, a software that identifies ligand-receptor pairs between different cell types present in scRNAseq data (43). This analysis identified several potential (high statistical significance) ligand-receptor pairs present in different pituitary lineages (Fig. 5*A*). Corticotropes (C) and gonadotropes (G) form homotypic networks (29) and accordingly, CellPhone revealed 10 potential C-C and 12 potential G-G ligand-receptor pairs (Fig. 5*A*, left). Some of the genes potentially involved in homo-/hetero-typic interactions were downregulated in HT corticotropes (Fig. 4*D* and Fig. 5*A* in red). The ligand-receptor pairs involving these genes are lost in HT samples (Fig. 5*A*, right), validating the analysis. Thus, the interaction pair involving secreted heparin-binding growth factor Ptn and receptor protein tyrosine phosphatase Ptprz1, a candidate for homotypic C-C communication is lost in HT samples because *Ptprz1* is downregulated in HT corticotropes (Fig. 4*D*). Tpit may thus play a role in homotypic C-C interactions. CellPhone analyzes also revealed candidates for heterotypic interactions, including some that are *Tpit* dosage sensitive. For instance, the interaction between Ptn and the plexin transmembrane receptor Plxnb2 potentially involved in C-G communication is lost in HT because *Plxnb2* is downregulated in HT corticotropes (Fig. 4*D*). In agreement with the observed preferential contacts between corticotropes and somatotropes (S), we identified 11 C-S/S-C ligand-receptor pairs. While most of these interaction pairs are conserved in HT mice, the interaction pair involving corticotrope-expressed FGF1 ligand and somatotrope TGFBR3 co-receptor is lost in HT samples (Fig. 5, red box) because

FGF1 is downregulated in *Tpit*-HT corticotropes (Fig. 4*D*). On the other hand, a novel interaction pair involving Bdnf-Ntrk2 appeared in HT, suggesting compensatory feedback. Indeed, both *Bdnf* and *Ntrk2* are upregulated in HT corticotropes (Fig. 4*D* and *SI* Dataset 1) and *Bdnf* is also upregulated in HT somatotropes (Fig. 4*E* and *SI* Dataset 3).

While the coreceptor *TGFBR3* shows broad expression within the pituitary, with the highest levels in gonadotropes and somatotropes, *FGF1* is only expressed in PSCs and Tpit-positive cells, corticotropes and melanotropes (Fig. 5*B* and *SI Appendix,* S5*A*). The expression of *FGF1* is low and uniform in early development but increases in the adult, while *TGFBR3* shows progressive increase in expression during development, with an onset coinciding with differentiation (*SI Appendix,* S5*B*). To visualize the effects of *Tpit* dosage on *FGF1* expression in corticotropes, we aggregated WT and HT clusters. While cells roughly cluster together, a clear segregation between WT and HT corticotropes was evident at closer view on the UMAP (Fig. 5*C*). *FGF1* appeared to be mostly expressed in WT cells (Fig. 5*D*, upper part) and DEG analysis revealed a 2.6x reduction in HT corticotropes (*SI Appendix,* Fig. S5*C*), which taken with the above, suggests that *FGF1* is a Tpit target gene. Using phospho-ERK1/2 (p-ERK) labeling as a readout of FGF1 signaling (44), we observed some p-ERK-positive cells (in particular close to corticotropes) in WT pituitaries and a sharp decrease of labeling in *Tpit*-HT pituitaries (Fig. 5*E* and *SI Appendix,* Fig. S5*D*). Tpit ChIPseq data (45) confirmed Tpit recruitment at the *FGF1* locus in AtT-20 corticotrope cells. Three Tpit recruitment peaks are present within *FGF1* intron B (Fig. 5*F*). These Tpit sites have features of enhancers, as revealed by H3K4me1 and P300 recruitment, as well as chromatin accessibility

(ATAC) assays (Fig. 5*F*). Importantly, 2 out of 3 putative *FGF1* enhancers are accessible as assessed by ATACseq in Tpit-positive (corticotropes) cells, but not in Tpit-negative gonadotropes, suggesting these are Tpit-dependent cell specific enhancers (Fig. 5*F*). Finally, a perfect palindromic Tpit response element is present under the #1 (largest) Tpit peak (Fig. 5*F*) and Tpit recruitment was confirmed at this location by ChIP-qPCR (*SI Appendix,* Fig. S5*E*). Further, a 500 bp fragment encompassing this region behaved as a bona fide Tpit-responsive enhancer in a luciferase reporter assay (*SI Appendix,* Fig. S5*F*). Similar observations were made for several other corticotrope or cortico/melanotrope specific genes (*SI Appendix,* Fig. S5*G* and *H*).

In summary, Tpit may regulate both homo- and hetero-typic cell-cell interactions in the pituitary. In particular, *FGF1* appears as a direct Tpit target gene putatively involved in corticotrope-somatotrope communication.

***FGF1* knockout phenocopies *Tpit*-dependent pituitary hypoplasia and GH deficiency.** We generated *FGF1* knockout mice to evaluate the putative role of FGF1 in the pituitary phenotype of *Tpit*-deficient mice. Since *FGF1* transcription is directed by at least three different promoters (27), we first determined which promoter is active in pituitary POMC cells. RNAseq analyses of sorted corticotropes showed that the first *FGF1* exon to be transcribed is exon B, indicating the use of promoter B. Therefore, we deleted by CRISPR a 1031 bp region comprising the *FGF1* promoter and exon B (*SI Appendix,* Fig. S6*A*). Western blot confirmed the loss of FGF1 in knockout mice (Fig. 6*A*). We observed a weight increase in knockout mice (*SI Appendix,* Fig. S6*B*), in

agreement with previous reports on the metabolic role of FGF1 in white adipose tissue (27, 46).

Interestingly, *FGF1* knockout APs appear smaller (Fig. 6*B*) and DNA content quantitation confirmed a reduced cell number in knockout AP like in *Tpit*-KO (Fig. 6*C*). We next assessed by Ki67 labelling the pituitary proliferation rate at three weeks, an age when slower proliferation is observed in *Tpit*-KO (Fig. 1 *E* and *F*), and indeed observed reduced proliferation index in *FGF1* knockouts compared to WT (Fig. 6 *D* and *E*). Further, as in *Tpit* knockouts, the percentage of GH-positive cells is reduced in *FGF1*-KO, (Fig. 6 *F* and *G*). Finally, two markers of GH action, hepatic IGF1 levels and tail length (47), are reduced in *FGF1*-deficient mice, indicative of reduced GH activity (Fig. 6 *H* and *I*). Collectively, these results show that *FGF1* inactivation phenocopies pituitary hypoplasia and GH-dependent growth retardation observed in *Tpit* knockout mice, supporting the idea that Tpit-dependent corticotrope-somatotrope communication is mediated through FGF1.

Discussion

Although all pituitary endocrine cell types are present at birth, pituitary development continues during the first postnatal weeks. During this period, a number of quantitative (proliferation) and qualitative changes (maturation, such as the Tpit-dependent enhancement of translation and secretory organellogenesis (17)) take place in order to fulfill the needs for high-capacity hormone production. At the end of fetal life, hormone-positive cells represent only 30% of AP cells but this proportion increases to 40% at birth, to 60% at day 5, to 80% at day 10 and to 90% at day 30 (48). During the same

period, overall pituitary volume increases ten times (13). Postnatal pituitary development is very dynamic, and the underlying molecular mechanisms are just beginning to be elucidated. While in early postnatal pituitary cell expansion derives from Sox2+ cells (49), later (P14) pituitary proliferation comes from committed progenitors that are negative for the stem cell marker Sox2 and negative for hormones. The first 3 weeks after birth correspond to the fastest pituitary postnatal growth wave (21) that is characterized by the highest proliferation index and a reduction of the stem cell population proportion (50). During this period, WNT signaling provided by Sox2-positive PSC stimulates proliferation of progenitor cells (21). By the age of 3 weeks, pituitary cell types reach the adult proportions and organize in networks, while the gland continues to growth but at slower pace. In the present study, we have seized the opportunity provided by the adult phenotype of *Tpit*$^{-/-}$ mice that exhibit hypoplasia and growth delays to address how different cell networks may communicate with each other during postnatal pituitary organogenesis. Until 3 weeks of age, the overall AP organization of *Tpit*-deficient mice appears normal, but thereafter, *Tpit*-KO mice show important perturbations of pituitary architecture and size, with a particular impact on somatotropes. *Tpit* mutants have less somatotropes and these somatotropes are smaller, with less secretory granules, that are marginalized, and lose polarity toward capillaries. These perturbations are *Tpit* dosage-sensitive, suggesting they are direct consequences of *Tpit* deficiency rather than secondary to systemic Gc deficiency. Combined with the observation of intimate contacts between corticotropes and somatotropes, these results suggest corticotropes provide critical signals for somatotrope expansion and maturation. Single cell transcriptomics identified FGF1,

specifically expressed in corticotropes, as the best candidate for mediating corticotrope-somatotrope communication and involvement in the postnatal GH cell phenotype (Fig. 7*A*). Accordingly, *FGF1*-KO mice phenocopy AP hypoplasia and growth retardation observed in *Tpit*-deficient mice. Current models suggest FGFs could act both at transcriptional level, through the Ras/MAPK/PI3K/Akt signaling pathways and at the level of cytoskeleton, through PLCγ, to regulate cell morphology, migration, and adhesion (51-53) (Fig. 7*B*). FGF1 and its closest paralog FGF2 were originally identified in pituitary extracts (22, 23) as factors stimulating fibroblast proliferation (24, 25). The pituitary hypoplasia in *Tpit*-HT mice may therefore be a consequence of the 2.6x reduction of *FGF1* transcripts in corticotropes. Accordingly, several genes regulating cell proliferation are deregulated in somatotropes of *Tpit*-HT and -KO mice (Fig. 4*G*, *SI Appendix* S4 *B* and *C*). FGF1 produced by PSC could also participate to the postnatal pituitary expansion. In agreement with that hypothesis, PSC FGF1 level are slightly reduced in *Tpit*-KO mice (*SI Appendix* S5*C*). Consistently, the *TGFBR3* coreceptor is broadly expressed in pituitary cells (Fig. 5*B*). The major effect of FGF1 on somatotropes may reflect their intimate contacts with corticotropes as FGF1 is known to diffuse poorly and act locally (54).

Cell size (55, 56) and secretory granule trafficking/transport (57-59) may be modulated by the cytoskeleton. FGF1 could act on the cytoskeleton both at the transcriptional level, and directly. Several genes encoding components of the cytoskeleton are indeed deregulated, mostly downregulated, in somatotropes of *Tpit*-HT mice (*SI* Dataset 3). These include a major constituent of microtubules *Tubb6* (2x down), and myosins *Myo1d* (3x down), *Myo5b* (2.3x down) and *Myo3b* (3x up). In addition, tubulin *Tuba8*

(6.8x down), as well as genes encoding actin binding proteins *Actn1* (4x down), *Actn2* (2x up), *Ablim1* (2.6x up), *Ablim3* (3x down), *Fscn1* (3.5x down), *Phactr1* (2.6x up), *Phactr3* (3.4x down), other components or regulators of cytoskeleton (*Arhgef10l*: 2.9x down, *Fmnl3*: 2.3x up, *Pxn*: 2.8x down) or components of trafficking and vesicle-mediated transport (*Rab3c/Rab3d:* 2.2x down, *Rab6b*: 8x down, *Rab7b*: 3x down, *Rab15*: 2.3x down, *Rab17*: 14.6x down) are deregulated in somatotropes of *Tpit*-KO mice (*SI* Dataset 4). Collectively, these gene expression changes may contribute to cell size reduction and abnormal distribution of GH granules in somatotropes of *Tpit* mutant mice. GH dimerization is the first step of GH aggregation in granules and it requires Zn^{2+} ions (60). Hence, regulation of cellular zinc transport plays an important role for the regulated GH secretory pathway. Interestingly, the zinc transporter *Slc39a14/Zip14* is downregulated in GH cells of *Tpit*-KO mice (x4 down: and *SI Appendix* Fig. S4*B* and Dataset 4). This could contribute to smaller and fewer GH granules in *Tpit*-KO mice. Besides its role in GH aggregation, Slc39c14 is also involved in signaling through the GHRHR receptor (61). The reduced levels of Slc39a14 may therefore decrease the sensitivity of somatotropes to GHRH. As a result, the regulated GH secretory pathway would be affected at two levels: GH aggregation and GH secretion in response to GHRH.

Another well-known mitogen for GH cells is the hypothalamic factor GH releasing hormone (GHRH) (62). Indeed, transgenic mice expressing the human *GHRH* gene display a dramatic pituitary hyperplasia (63) while homozygous *little* (*lit/lit*) mice mutant for the *GHRH* receptor display postnatal GH cell hypoplasia (64). Moreover, GH cell maturation is also affected in *little* mice that have a severe reduction in GH granule size

and mislocalization to the cell periphery (margination) (65), resembling that observed in *Tpit* mutant mice (Fig. 3 *E*, *F*, *H* and *I*). While the corticotrope network mostly occupies the ventral part of the developing pituitary, GHRH mitogenic action is mostly exerted on the caudomedial region. Lin et al. proposed the existence of spatially distinct proliferating zones of GH cells, each regulated by a different factor (64). Therefore, it is tempting to speculate that there might be at least two populations of GH cells, sensitive to two different mitogens: FGF1 produced by corticotropes in the ventral part and GHRH released by hypothalamus in the caudomedian zone. It is interesting to note that scRNAseq indeed revealed two somatotrope populations (#1 and #2) with cluster #1 expressing 2.2x more GHRH receptor (GHRHR) mRNA and cluster #2 being more sensitive to the *Tpit* mutation (Fig. 5*C*). Notably, GHRHR is 2.8x downregulated in somatotropes of *Tpit*-KO mice (*SI Appendix* Fig. S4*B* and Dataset 4), which may reduce their response to GHRH mitogenic and secretagogue action and further contribute to the GH-deficiency phenotype.

In summary, our results demonstrate the importance of cell-cell communications for postnatal pituitary development and establish the corticotrope cell network as a pivotal source of FGF1 for regulation of pituitary architecture and size.

Materials and Methods

Mice. The generation and genotyping of *Tpit*-KO and POMC-eGFP reporter mice were described elsewhere (20, 35). *POMC*-KO mice originally generated by Yaswen et al. (40) were purchased from Jackson laboratory (B6.129X1-Pomc^{tm2Ute}/J strain, stock

number 008115). *FGF1* knockout mouse line featuring a 1031 bp deletion spanning the transcription start site (TSS) was generated using CRISPR-Cas9 system via the *i*-GONAD procedure (66). Briefly, recombinant Cas9 nuclease (IDT cat# 1081060) and two gRNA (crRNA and tracrRNA from IDT cat# 1072532) were pre-assembled into ribonucleoprotein (RNP) complexes and injected into ampulla of CD1 pregnant females at 0.7 days post conception, followed by electroporation. CRISPR-Cas9 guide RNA design tool from IDT were used to select gRNA. Genotyping primer and gRNA sequences are given in *SI Appendix,* Table S1. *Tpit*-KO mice were maintained in Balb/c genetic background, *POMC*-KO and POMC-eGFP mice in C57Bl/6 background and *FGF1*-KO mice in CD1 background. Each experiment was performed with control mice of the same genetic background as the mutants. Animal experimentations were approved by the IRCM Animal Care and Use Committee (protocol numbers 2021-13 JD and 2021-04 MK) in conformity with regulations of the Canadian Council on Animal Care.

Extraction of pituitary genomic DNA. Whole pituitaries, or anterior pituitaries, were first incubated in 1.5 ml tubes with proteinase K (PK, 60 µg/well) in 400 µl of PK-lysis buffer (0.5% SDS - 100 mM NaCl, 50 mM Tris, pH 7.5 - 1 mM EDTA) at 55°C, overnight. After a brief RNase treatment (10 µg/tube, RT, 15 min), samples were retreated with PK (20 µg/tube, 55°C, 1 h). Genomic DNA was then precipitated with 0.4 volumes of 7 M ammonium acetate (to reach a final concentration of 200 mM) – 0.7 volume of isopropanol (500 µl), washed with cold 70% ethanol and dissolved in 50-100 µl of 10 mM Tris, pH 8.0 at 55°C overnight. DNA was quantitated using TKO100

Fluorometer following the manufacturer's instructions (Hoefer Scientific Instruments). Pituitary cell number was inferred from the DNA content with the assumption that a diploid mouse cell contains ≈6 pg of DNA (≈$3x10^9$ bp per haploid genome).

Pituitary GH content. Pituitaries were dissected and kept frozen at -80°C in 1xPBS and GH contents were measured as previously described (67).

See also **Supplementary Methods and references in *SI Appendix* text**

Data availability. Sequencing data have been deposited with Gene Expression Omnibus (GEO) under accession number GSE227561.

ACKNOWLEDGMENTS. We are grateful to Alexandre Mayran and David Langlais for sharing their expertise on scRNAseq, to Jonathan Brière for model drawing, and to Michael Housset and Aurélio Balsalobre for their inputs throughout this work. We thank Simone Terouz and Yves Gauthier for help with histology and Tpit ChIP, respectively, Dominic Filion for the script allowing image analysis and Valérie Magoon for her expert secretarial assistance as well as the Small animal imaging platform of Montpellier (IPAM-BCM, certified to ISO9001). This work was supported by grants from Canadian Institutes of Health Research (CIHR FDN 154297), from the Agence Nationale de la Recherche (France-Bioimaging ANR-10-INBS-04, ANR-18-CE14-0017 and ANR-22-CE14-0001-01 to C.L. and P.M.) and by access to Compute Canada resources. K.K. was supported by CIHR and FRQS.

Authors contributions. K.K. and J.D. conceived and designed the experiments. K.K., K.S., C.L., H.C. and P.L.T. performed experiments. A.B. and A.G. performed bioinformatic analysis of scRNAseq data. Y.K and M.K. designed and performed CRISPR inactivation of *FGF1* in mice by *i*-GONAD technology. P.M. helped with the experimental design and interpretation of data. K.K. and J.D. wrote the manuscript.

Competing interests. The authors do not have any conflict of interests to declare.

1. J. Drouin, J. Brière, "Chap 1 - Pituitary Development" in The Pituitary (Fitfh Edition), S. Melmed, Ed. (2022), pp. 1-24.
2. T. Fauquier, K. Rizzoti, M. Dattani, R. Lovell-Badge, I. C. Robinson, SOX2-expressing progenitor cells generate all of the major cell types in the adult mouse pituitary gland. *Proc. Natl. Acad. Sci. USA* **105**, 2907-2912 (2008).
3. J. Chen *et al.*, The adult pituitary contains a cell population displaying stem/progenitor cell and early embryonic characteristics. *Endocrinology* **146**, 3985-3998 (2005).
4. J. Chen *et al.*, Pituitary progenitor cells tracked down by side population dissection. *Stem Cells* **27**, 1182-1195 (2009).
5. A. S. Gleiberman *et al.*, Genetic approaches identify adult pituitary stem cells. *Proc. Natl. Acad. Sci. USA* **105**, 6332-6337 (2008).
6. L. O'Hara, H. C. Christian, N. Jeffery, P. Le Tissier, L. B. Smith, Characterisation of a mural cell network in the murine pituitary gland. *J Neuroendocrinol* **32**, e12903 (2020).
7. K. M. Scully, M. G. Rosenfeld, Pituitary development: regulatory codes in mammalian organogenesis. *Science* **295**, 2231-2235 (2002).
8. B. Lamolet *et al.*, A pituitary cell-restricted T-box factor, Tpit, activates POMC transcription in cooperation with Pitx homeoproteins. *Cell* **104**, 849-859 (2001).
9. H. A. Ingraham *et al.*, A tissue-specific transcription factor containing a homeodomain specifies a pituitary phenotype. *Cell* **55**, 519-529 (1988).
10. S. Li *et al.*, Dwarf locus mutants lacking three pituitary cell types result from mutations in the POU-domain gene pit-1. *Nature* **347**, 528-533 (1990).
11. C. E. Stallings, J. Kapali, B. S. Ellsworth, Mouse Models of Gonadotrope Development. *Prog Mol Biol Transl Sci* **143**, 1-48 (2016).
12. Y. Taniguchi, S. Yasutaka, R. Kominami, H. Shinohara, Proliferation and differentiation of rat anterior pituitary cells. *Anat. Embryol. (Berl)* **206**, 1-11 (2002).
13. E. Carbajo-Pérez, Y. G. Watanabe, Cellular proliferation in the anterior pituitary of the rat during the postnatal period. *Cell Tissue Res* **261**, 333-338 (1990).
14. R. Kominami, S. Yasutaka, Y. Taniguchi, H. Shinohara, Proliferating cells in the rat anterior pituitary during the postnatal period: immunoelectron microscopic observations using monoclonal anti-bromodeoxyuridine antibody. *Histochem Cell Biol* **120**, 223-233 (2003).
15. H. L. Burrows, K. R. Douglas, A. F. Seasholtz, S. A. Camper, Genealogy of the Anterior Pituitary Gland: Tracing a Family Tree. *Trends Endocrinol. Metab* **10**, 343-352 (1999).
16. Y. Taniguchi, R. Kominami, S. Yasutaka, Y. Kawarai, Proliferation and differentiation of pituitary corticotrophs during the fetal and postnatal period: a quantitative immunocytochemical study. *Anat. Embryol. (Berl)* **201**, 229-234 (2000).
17. K. Khetchoumian *et al.*, Pituitary cell translation and secretory capacities are enhanced cell autonomously by the transcription factor Creb3l2. *Nature Communications* **10**, 3960 (2019).
18. Y. Taniguchi, S. Yasutaka, R. Kominami, H. Shinohara, Proliferation and differentiation of pituitary somatotrophs and mammotrophs during late fetal and postnatal periods. *Anat Embryol (Berl)* **204**, 469-475 (2001).
19. E. Laporte, A. Vennekens, H. Vankelecom, Pituitary Remodeling Throughout Life: Are Resident Stem Cells Involved? *Front Endocrinol (Lausanne)* **11**, 604519 (2020).

20. P. L. Lavoie, L. Budry, A. Balsalobre, J. Drouin, Developmental Dependence on NurRE and EboxNeuro for Expression of Pituitary POMC. *Mol. Endocrinol* **22**, 1647-1657 (2008).
21. J. P. Russell *et al.*, Pituitary stem cells produce paracrine WNT signals to control the expansion of their descendant progenitor cells. *eLife* **10** (2021).
22. A. G. Gambarini, H. A. Armelin, Purification and partial characterization of an acidic fibroblast growth factor from bovine pituitary. *J Biol Chem* **257**, 9692-9697 (1982).
23. D. Gospodarowicz, Purification of a fibroblast growth factor from bovine pituitary. *J Biol Chem* **250**, 2515-2520 (1975).
24. D. Gospodarowicz, J. S. Moran, Mitogenic effect of fibroblast growth factor on early passage cultures of human and murine fibroblasts. *J Cell Biol* **66**, 451-457 (1975).
25. D. Gospodarowicz, J. Weseman, J. Moran, Presence in brain of a mitogenic agent promoting proliferation of myoblasts in low density culture. *Nature* **256**, 216-219 (1975).
26. D. L. Miller, S. Ortega, O. Bashayan, R. Basch, C. Basilico, Compensation by fibroblast growth factor 1 (FGF1) does not account for the mild phenotypic defects observed in FGF2 null mice. *Mol Cell Biol* **20**, 2260-2268 (2000).
27. J. W. Jonker *et al.*, A PPARγ-FGF1 axis is required for adaptive adipose remodelling and metabolic homeostasis. *Nature* **485**, 391-394 (2012).
28. X. Bonnefont *et al.*, Revealing the large-scale network organization of growth hormone-secreting cells. *Proc. Natl. Acad. Sci. USA* **102**, 16880-16885 (2005).
29. L. Budry *et al.*, Related pituitary cell lineages develop into interdigitated 3D cell networks. *Proc. Natl. Acad. Sci. USA* **108**, 12515-12520 (2011).
30. D. J. Hodson *et al.*, Existence of long-lasting experience-dependent plasticity in endocrine cell networks. *Nat Commun* **3**, 605 (2012).
31. P. Mollard, D. J. Hodson, C. Lafont, K. Rizzoti, J. Drouin, A tridimensional view of pituitary development and function. *Trends Endocrinol Metab* **23**, 261-269 (2012).
32. P. R. Le Tissier *et al.*, Anterior pituitary cell networks. *Front Neuroendocrinol* **33**, 252-266 (2012).
33. P. K. Nakane, Classifications of anterior pituitary cell types with immunoenzyme histochemistry. *J Histochem. Cytochem* **18**, 9-20 (1970).
34. Y. G. Watanabe, An immunohistochemical study on the mouse adenohypophysis with reference to the spatial relationship between GH cells and other types of hormone-producing cells. *Anat. Embryol. (Berl)* **172**, 277-280 (1985).
35. A. M. Pulichino *et al.*, Tpit determines alternate fates during pituitary cell differentiation. *Genes Dev* **17**, 738-747 (2003).
36. A. Mayran *et al.*, Pioneer and nonpioneer factor cooperation drives lineage specific chromatin opening. *Nature Communications* **10**, 3807 (2019).
37. A. M. Pulichino *et al.*, Human and mouse Tpit gene mutations cause early onset pituitary ACTH deficiency. *Genes Dev* **17**, 711-716 (2003).
38. S. Vallette-Kasic *et al.*, Congenital isolated adrenocorticotropin deficiency: an underestimated cause of neonatal death, explained by TPIT gene mutations. *J. Clin. Endocrinol. Metab* **90**, 1323-1331 (2005).
39. C. Couture *et al.*, Phenotypic homogeneity and genotypic variability in a large series of congenital isolated ACTH deficiency patients with TPIT gene mutations. *J Clin Endocrinol Metab* **97**, 486-495 (2012).

40. L. Yaswen, N. Diehl, M. B. Brennan, U. Hochgeschwender, Obesity in the mouse model of pro-opiomelanocortin deficiency responds to peripheral melanocortin. *Nat. Med* **5**, 1066-1070 (1999).
41. C. Lafont *et al.*, Cellular in vivo imaging reveals coordinated regulation of pituitary microcirculation and GH cell network function. *Proc. Natl. Acad. Sci. USA* **107**, 4465-4470 (2010).
42. L. McInnes, J. Healy, J. J. a. p. a. Melville, Umap: Uniform manifold approximation and projection for dimension reduction. (2018).
43. M. Efremova, M. Vento-Tormo, S. A. Teichmann, R. Vento-Tormo, CellPhoneDB: inferring cell-cell communication from combined expression of multi-subunit ligand-receptor complexes. *Nat Protoc* **15**, 1484-1506 (2020).
44. R. T. Böttcher, C. Niehrs, Fibroblast growth factor signaling during early vertebrate development. *Endocr Rev* **26**, 63-77 (2005).
45. L. Budry *et al.*, The selector gene Pax7 dictates alternate pituitary cell fates through its pioneer action on chromatin remodeling. *Genes & Development* **26**, 2299-2310 (2012).
46. G. Sancar *et al.*, FGF1 and insulin control lipolysis by convergent pathways. *Cell Metab* **34**, 171-183.e176 (2022).
47. L. R. Donahue, W. G. Beamer, Growth hormone deficiency in 'little' mice results in aberrant body composition, reduced insulin-like growth factor-I and insulin-like growth factor-binding protein-3 (IGFBP-3), but does not affect IGFBP-2, -1 or -4. *J Endocrinol* **136**, 91-104 (1993).
48. G. Smets *et al.*, Ontogeny of hormone-secreting cells of the rat pituitary gland: an immunocytochemical study on dissociated cells. *Histochem J* **21**, 337-342 (1989).
49. X. Zhu, J. Tollkuhn, H. Taylor, M. G. Rosenfeld, Notch-Dependent Pituitary SOX2(+) Stem Cells Exhibit a Timed Functional Extinction in Regulation of the Postnatal Gland. *Stem cell reports* **5**, 1196-1209 (2015).
50. L. Gremeaux, Q. Fu, J. Chen, H. Vankelecom, Activated phenotype of the pituitary stem/progenitor cell compartment during the early-postnatal maturation phase of the gland. *Stem Cells Dev* **21**, 801-813 (2012).
51. A. M. Vallés, G. C. Tucker, J. P. Thiery, B. Boyer, Alternative patterns of mitogenesis and cell scattering induced by acidic FGF as a function of cell density in a rat bladder carcinoma cell line. *Cell Regul* **1**, 975-988 (1990).
52. S. Yang *et al.*, FGF signaling directs myotube guidance by regulating Rac activity. *Development* **147** (2020).
53. C. M. Teven, E. M. Farina, J. Rivas, R. R. Reid, Fibroblast growth factor (FGF) signaling in development and skeletal diseases. *Genes Dis* **1**, 199-213 (2014).
54. Y. Xie *et al.*, FGF/FGFR signaling in health and disease. *Signal Transduct Target Ther* **5**, 181 (2020).
55. S. F. Pedersen, E. K. Hoffmann, J. W. Mills, The cytoskeleton and cell volume regulation. *Comp Biochem Physiol A Mol Integr Physiol* **130**, 385-399 (2001).
56. W. F. Marshall *et al.*, What determines cell size? *BMC Biol* **10**, 101 (2012).
57. T. Senda *et al.*, Ultrastructural and immunocytochemical studies on the cytoskeleton in the anterior pituitary of rats, with special regard to the relationship between actin filaments and secretory granules. *Cell Tissue Res* **258**, 25-30 (1989).
58. T. Senda, Mechanisms of secretory granule transport and exocytosis in anterior pituitary cells. *Ital J Anat Embryol* **100 Suppl 1**, 219-229 (1995).

59. R. Rudolf, T. Salm, A. Rustom, H. H. Gerdes, Dynamics of immature secretory granules: role of cytoskeletal elements during transport, cortical restriction, and F-actin-dependent tethering. *Mol Biol Cell* **12**, 1353-1365 (2001).
60. V. Petkovic, M. C. Miletta, P. E. Mullis, From endoplasmic reticulum to secretory granules: role of zinc in the secretory pathway of growth hormone. *Endocr Dev* **23**, 96-108 (2012).
61. S. Hojyo *et al.*, The zinc transporter SLC39A14/ZIP14 controls G-protein coupled receptor-mediated signaling required for systemic growth. *PloS one* **6**, e18059 (2011).
62. N. Billestrup, L. W. Swanson, W. Vale, Growth hormone-releasing factor stimulates proliferation of somatotrophs in vitro. *Proc Natl Acad Sci U S A* **83**, 6854-6857 (1986).
63. K. E. Mayo *et al.*, Dramatic pituitary hyperplasia in transgenic mice expressing a human growth hormone-releasing factor gene. *Mol Endocrinol* **2**, 606-612 (1988).
64. S. C. Lin *et al.*, Molecular basis of the little mouse phenotype and implications for cell type-specific growth. *Nature* **364**, 208-213 (1993).
65. D. B. Wilson, D. P. Wyatt, R. M. Gadler, C. A. Baker, Quantitative aspects of growth hormone cell maturation in the normal and little mutant mouse. *Acta Anat (Basel)* **131**, 150-155 (1988).
66. C. B. Gurumurthy *et al.*, Creation of CRISPR-based germline-genome-engineered mice without ex vivo handling of zygotes by i-GONAD. *Nat Protoc* **14**, 2452-2482 (2019).
67. F. J. Steyn *et al.*, Development of a method for the determination of pulsatile growth hormone secretion in mice. *Endocrinology* **152**, 3165-3171 (2011).
68. A. Mayran *et al.*, Pioneer factor Pax7 deploys a stable enhancer repertoire for specification of cell fate. *Nat Genet* **50**, 259–269 (2018).
69. D. Langlais, C. Couture, G. Sylvain-Drolet, J. Drouin, A pituitary-specific enhancer of the POMC gene with preferential activity in corticotrope cells. *Mol. Endocrinol* **25**, 348-359 (2011).

Figure legends

Fig. 1. Smaller anterior pituitary lobes (AL) in *Tpit*$^{-/-}$ mutant mice. (*A*) Hematoxylin and eosin staining of sections from adult (3-month-old) WT and *Tpit*-KO mouse pituitaries. Scale bar: 500 µm. IL, intermediate lobe. PL, posterior lobe. (*B*) AL genomic DNA contents (means ± SEM, n = 3-7 ALs/genotype) from *Tpit*-heterozygous (HT: blue), *Tpit*-knockout (KO: red) and *POMC*-KO (purple) mice relative to their WT littermate controls. Data are normalized for body weights. (*C-D*) Postnatal pituitary growth. Pituitary genomic DNA contents of WT (black), *Tpit*-HT (blue) and *Tpit*-KO (red) male (*C*) and female (*D*) mice. The right Y axis reports total pituitary genomic DNA content (means ± SEM, n = 3-28 mice/group), while the left Y axis corresponds to the deduced total number of cells per pituitary. The X axis represent the age in days. (*E-F*) Ki67 immunostaining and quantitation (means ± SEM, n = 2-8 mice/group) of P5 and 3-week-old WT and *Tpit*-HT pituitary sections from males and females. Scale bars: 200 µm. Demarcations between pituitary lobes (anterior: AL, intermediate: IL, posterior: PL) are indicated by white dashed lines. All graphs were done using GraphPad Prism 9 and statistical significance was determined using bilateral Student's t-test. **P* < 0.05, ***P* < 0.005, ****P* < 0.0005 vs WT.

Fig. 2. Growth hormone (GH) deficiency in Tpit mutant mice. (*A-F*) Intimate contacts between corticotrope and somatotrope cells in the adult anterior pituitary. (*A*) Visualization of corticotrope and somatotrope contacts using eGFP for visualizing corticotropes (POMC cells, green) or immunofluorescence against GH (magenta). (*B-D*) Homotypic corticotrope (green) interactions do not show strong β-Catenin staining (*B*,

arrow 1), whereas tight contacts (< 0.5 µm) marked by β-Catenin staining are observed between somatotropes (*C*, arrow 2) or between somatotropes (grey) and corticotropes (*D*, magenta, arrow 3). Scale bars: 20 µm. (*E-F*) Surfacing of eGFP/ACTH (green), β-Catenin (yellow), and GH (purple) signals illustrating (*E*) and quantifying (*F*) intimate corticotrope/β-Catenin/somatotrope contacts. (*F*) Quantification of colocalization of β-Catenin signal with either POMC or GH, and colocalization of β-Catenin within POMC cells in close contact with GH cells [15 z-stacks of images; 4 animals]. (*G-I*) Growth hormone related defects in *Tpit* mutant mice. (*G*) Real-time quantitative PCR (RT-qPCR) assessment of GH and POMC mRNA levels in 3-month-old normal (WT), heterozygous (HT) and *Tpit*-deficient (KO) males (left) and females (right). Relative mRNA levels were normalized to *TBP* mRNA and represented as fraction of WT levels. Data represent averages (± SEM) of 5-6 mice per genotype. (*H*) *Tpit* dosage-dependent reduction of pituitary GH content. GH contents in 3-month-old mice were measured as described (67). Data represent averages (± SEM) of 5 mice per genotype. (*I*) RT-qPCR analyzes of GH-dependent liver *IGF1* mRNA levels (normalized relative to *TBP* mRNA) in males (left) and females (right) of indicated *Tpit* genotypes. Data represent averages ± SEM of 5-6 mice per genotype. (*J*) GH immunostaining on 3-week-old WT and *Tpit*-HT pituitary sections. Scale bars: 150 µm. (*K*) Percentage of GH-positive cells (means ± SEM, n = 2-8 mice/group) in WT and *Tpit*-HT male and female pituitaries. (*L-M*) Mouse length measurements (body and tail means ± SEM, n = 7-15 mice/group) indicate shorter size in *Tpit*-KO males and females. Statistical significance was determined using RM one-way ANOVA in Prism (GraphPap) or bilateral Student's t-test in Microsoft Excel. **P* < 0.05, ***P* < 0.005, ****P* < 0.0005, *****P* < 0.0001 *vs* WT.

Fig. 3. Somatotrope ultrastructural abnormalities in *Tpit* mutant mice. (*A*-*I*) Electron micrographs of somatotropes. (*A*-*C*) WT somatotropes exhibiting secretory granule polarity towards blood vessels (Cap), as shown by the blue arrow in (*A*). (*D*-*F*) *Tpit*$^{+/-}$ somatotropes showing less granule polarity with an example (*F*) of secretory granules margination. (*G*-*I*) *Tpit*$^{-/-}$ somatotropes showing loss of secretory granule polarity towards capillaries, whilst (I) shows two somatotropes with granule margination. Scale bars: 2 µm. S = somatotrope, Cap = capillary. (*J*-*L*) Quantification of cytoplasmic area (*J*) granule area (*K*) and granule diameter (*L*) in *Tpit* WT, HT and KO somatotropes. Data are means ± SEM (n = 4 for all groups) **P* < 0.05, ***P* < 0.01 *vs* WT.

Fig. 4. ScRNAseq analyzes of WT, *Tpit*-HT and *Tpit*-KO pituitaries. (*A*) UMAP representation of different pituitary cell clusters. Detailed identification of clusters is reported in *SI Appendix* Fig. S3*A*-*B*. (*B*) Cell type proportions (%) per genotype determined in scRNAseq. (*C*) Number of differentially expressed genes (DEG) for each cell cluster of *Tpit*-HT compared to WT cells. Bars represent the number of genes downregulated (yellow) or upregulated (blue) in *Tpit*-HT *vs* WT cells using the following criteria: $1 \leq \log_2 FC \leq -1$, $-\log_{10}P > 4$. (*D*) Volcano plot showing DEG analysis between WT and *Tpit*-HT corticotrope cells. Examples of genes encoding ligands/receptors up- (left) or down- (right) regulated in HT corticotropes are shown on the graph. 41 out of 68 downregulated genes correspond to corticotrope-signature genes as determined by Seurat (*SI* Dataset 2). (*E*-*G*) Deregulation of the MAPK/Ras and PI3K-Akt pathways in *Tpit*-HT somatotropes. (*E*) Volcano plot showing DEG analysis of WT and *Tpit*-HT somatotrope cells (cluster #2). Examples of genes of the Ras/MAPK pathway are shown on the graph by arrows. (*F*) Gene ontology analysis of DEG in *Tpit*-HT

somatotropes (cluster #2) showing deregulation of the MAPK/Ras and PI3K pathways. The size and color of the dots are proportional to the size of the category. (*G*) Dot plot showing expression of select genes of the MAPK/Ras and PI3K pathways in WT, *Tpit*-HT and *Tpit*-KO somatotropes (WT and HT cluster #2, KO cluster #5). The dot diameters reflect the number of cells expressing a given gene, while the intensity of its color is proportional to the mean expression level of the gene within the cluster.

Fig. 5. *FGF1* is a cortico/melanotrope-specific, Tpit-dependent gene for corticotrope-somatotrope communication. (*A*) Most significant ligand-receptor interactions between different cell types identified in WT (left) and *Tpit*-HT (right) scRNAseq samples using CellPhoneDB (43). The mean expression and *p* values of different ligand-receptor pairs are indicated by circle color and size, respectively. Interacting molecules downregulated in *Tpit*-HT are shown in red at left, while those upregulated in *Tpit*-HT are in blue at right. The gray vertical boxes show interaction pairs between corticotropes and somatotropes. Horizontal boxes indicate interactions lost (*FGF1*, in red) or gained (*BDNF*, in blue) in *Tpit*-HT. Other homotypic (*Ptprz1*) or heterotypic (*Plxnb2*) corticotrope interactions that are lost in *Tpit*-HT are shown by red arrows. (*B-D*) *FGF1* expression in pituitary cells.

(*B*) Visualization of *FGF1* and *TGFBR3* expression in WT pituitary cells. While *FGF1* is expressed in the two POMC lineages (corticotropes and melanotropes) and pituitary stem cells (PSC), *TGFBR3* is broadly expressed in pituitary, with the strongest expression in gonadotropes and somatotropes. The numbers in parentheses indicate the normalized expression levels for each cluster. (*C, D*) UMAP aggregation of WT and *Tpit*-HT corticotrope clusters showing spatial segregation of the two clusters. This

segregation reflects transcriptomic changes, as exemplified by expression of *FGF1* (*C*) that is mostly expressed on the upper (WT) part of the overlay cluster. (*E*) P-ERK1/2 staining on WT and *Tpit*-HT 3-week-old pituitaries and quantifications showing greater labeling in WT pituitaries. White circles show two examples of p-ERK1/2-positive cells next to ACTH-positive cells (corticotropes) in WT pituitary. Quantitations of these occurrences in WT and HT pituitaries is reported below micrographs. Pituitary overviews of these stainings are presented in *SI Appendix* S5*D*. Scale bar: 20 µm. (*F*) *FGF1* is a direct Tpit target gene. RNAseq (top) and ATACseq (bottom) profiles at the *FGF1* locus in FACS-sorted cortico- and gonado-trope mouse cells (68). ChIPseq profiles (middle) in AtT-20 corticotrope cells (45, 68) showing three Tpit recruitment peaks (#1-3) exhibiting active enhancer marks, namely bimodal H3K4me1, P300 and ATAC peaks in *FGF1* intron B. A palindromic Tpit response element sequence (45, 69) is present under peak #1.

Fig. 6. *FGF1* gene inactivation phenocopies pituitary hypoplasia and growth retardation observed in *Tpit*-KO mice. (*A*) Western blot analysis of kidney protein extracts (200 µg) from two WT and two *FGF1*-KO mutant mice revealed with an anti-FGF1 monoclonal antibody. The arrow indicates the expected size of FGF1 migration, the asterisk shows a nonspecific band used as loading control. (*B*-*C*) Smaller anterior pituitary lobes (AL) in *FGF1*$^{-/-}$ mutant mice. (*B*) Hematoxylin and eosin staining of sections from adult (3-month-old) WT and *FGF1*-KO mouse pituitaries. Scale bar: 500 µm. IL, intermediate lobe. PL, posterior lobe. (*C*) AL genomic DNA contents (means ± SEM, n = 4-12 ALs/genotype) from *FGF1*-KO (light red) and *Tpit*-KO (red) mice relative to their WT littermate controls. Data were normalized for body weights. (*D*-*E*) Reduced proliferation

762 rate in *FGF1*-KO pituitaries at 3-weeks. (*D*) Ki67 immunostaining of 3-weeks old WT
763 and *FGF1*-KO pituitary sections. Scale bars: 150 µm. Demarcations between pituitary
764 lobes (anterior: AL, intermediate: IL, posterior: PL) are indicated by white dashed lines.
765 (*E*) Percentages (means ± SEM, n = 3-4 mice/group) of Ki67-positive cells in WT and
766 *FGF1*-KO male and female pituitaries. (*F-I*) Reduced GH signaling in *FGF1*-KO mice.
767 (*F*) GH immunostaining on 3-week-old WT and *Tpit*-HT pituitary sections. Scale bars: 50
768 µm. (*G*) Percentage of GH-positive cells (means ± SEM, n = 3-4 mice/group) in WT
769 (grey) and *FGF1*-KO (light red) male and female pituitaries. (*H*) RT-qPCR analyzes of
770 GH-dependent liver *IGF1* mRNA levels (normalized relative to *TBP* mRNA) in *FGF1*-KO
771 (light red) mice compared to WT controls (grey). Data represent averages ± SEM of 5-6
772 mice per genotype. (*I*) Mouse length measurements (tail means ± SEM, n = 12-20
773 mice/group) indicating shorter tail size in *FGF1*-KO mice (light red) compared to WT
774 controls (grey). All graphs were done using GraphPad Prism 9 and statistical
775 significance was determined using bilateral Student's t-test. **P* < 0.05, ***P* < 0.005, ****P*
776 < 0.0005 *vs* WT.

777 **Fig. 7.** Tpit and FGF1 coordinate late postnatal pituitary organogenesis. (*A*) Schematic
778 representation of corticotrope-somatotrope-vasculature unit in WT and *Tpit*-KO
779 pituitaries. There are intimate contacts between corticotropes and somatotropes and
780 between somatotropes and capillaries, while corticotropes are interacting with the
781 capillaries via cytonemes (29). GH secretory granules in somatotropes accumulate
782 mainly next to capillaries. In *Tpit*-KO mice, somatotropes are smaller, with less and
783 smaller GH granules, that lose polarity. (*B*) Proposed model on the role of corticotrope
784 secreted FGF1 in postnatal pituitary development. Ras/MAPK/PI3K/Akt mediated

785 actions of FGF1 act on somatotrope proliferation (mitogenic effect), growth (cell size),
786 GH granule size and localization through transcriptional regulation of genes involved in
787 corresponding pathways. FGF1 could also directly act on the cytoskeleton of
788 somatotropes via the PLCγ pathway.

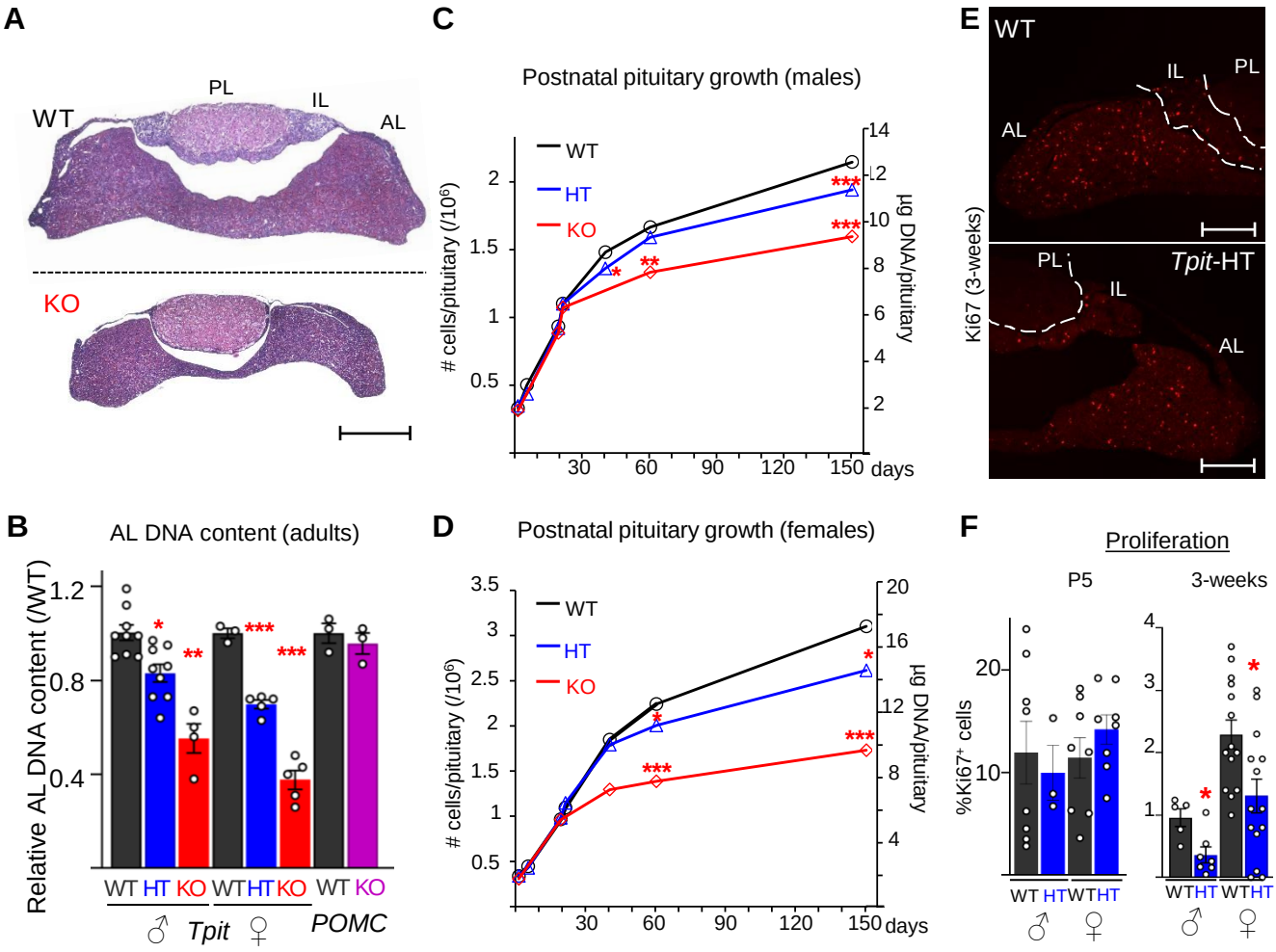
A
WT
PL
IL
AL
KO
B
AL DNA content (adults)
Relative AL DNA content (/WT)
1.2
0.8
0.4
WT HT KO WT HT KO WT KO
♂ Tpit ♀ POMC
C
Postnatal pituitary growth (males)
cells/pituitary (/10⁶)
µg DNA/pituitary
WT
HT
KO
30 60 90 120 150 days
D
Postnatal pituitary growth (females)
cells/pituitary (/10⁶)
µg DNA/pituitary
WT
HT
KO
30 60 90 120 150 days
E
WT
IL
PL
AL
Ki67 (3-weeks)
PL
IL
Tpit-HT
AL
F
Proliferation
P5
3-weeks
%Ki67⁺ cells
WT HT WT HT
♂ ♀
WT HT WT HT
♂ ♀

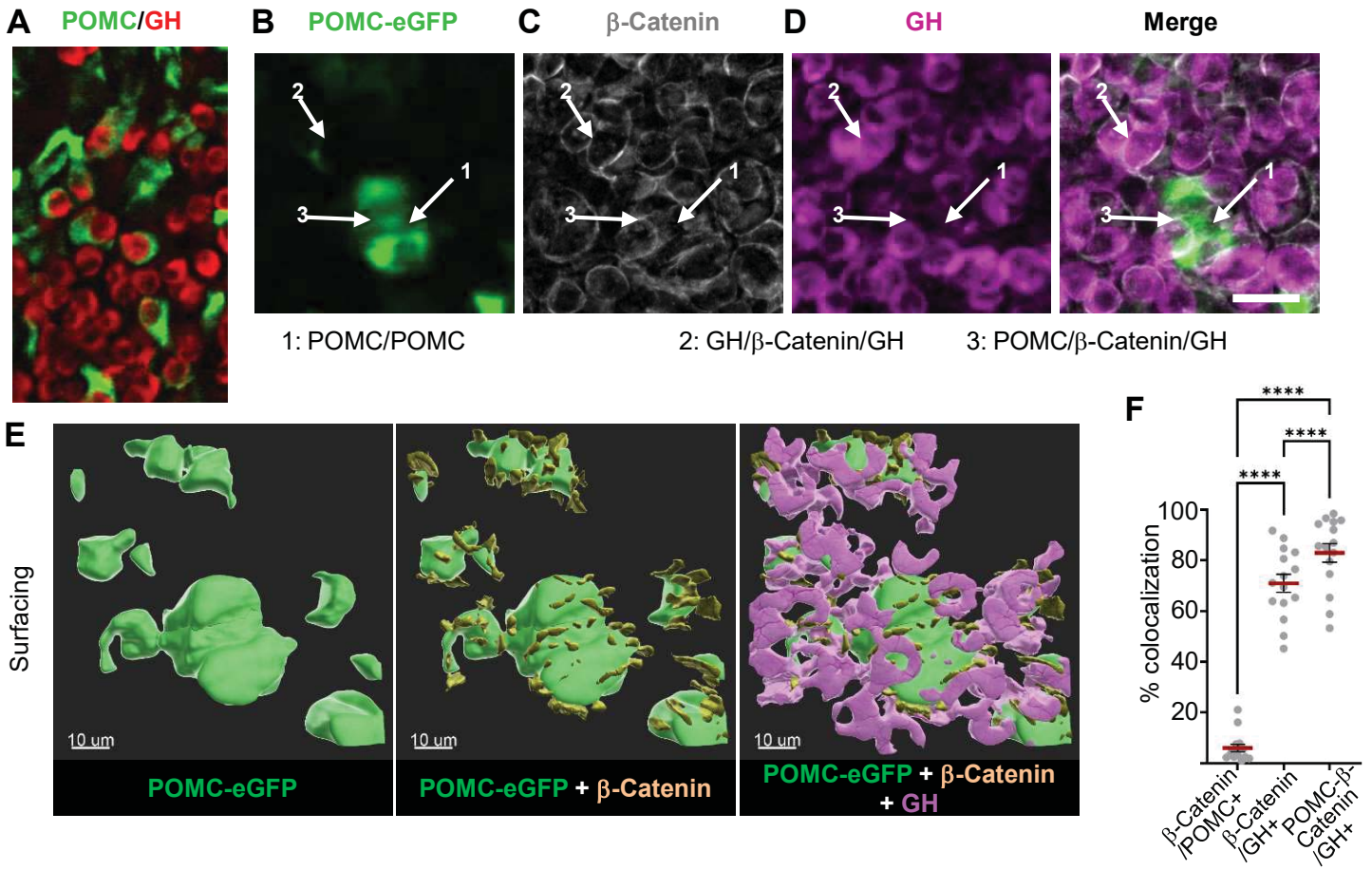
A POMC/GH
B POMC-eGFP
C β-Catenin
D GH
Merge
1: POMC/POMC
2: GH/β-Catenin/GH
3: POMC/β-Catenin/GH
E
Surfacing
10 um
POMC-eGFP
POMC-eGFP + β-Catenin
POMC-eGFP + β-Catenin + GH
F
% colocalization
β-Catenin /POMC+
β-Catenin /GH+
POMC-β-Catenin /GH+
G
GH/POMC expression (adults)
WT HT KO
Relative mRNA level (/WT)
GH
POMC
H
Pituitary GH content
µg GH/pituitary
I
Hepatic IGF1
Relative mRNA level (/WT)
J
GH
WT
Tpit HT
K
GH cell % (3-weeks)
%GH+ cells/DAPI
L
Body length (nose-to-anus)
Nose-to-anus length (mm)
M
Tail length
Tail length (mm)

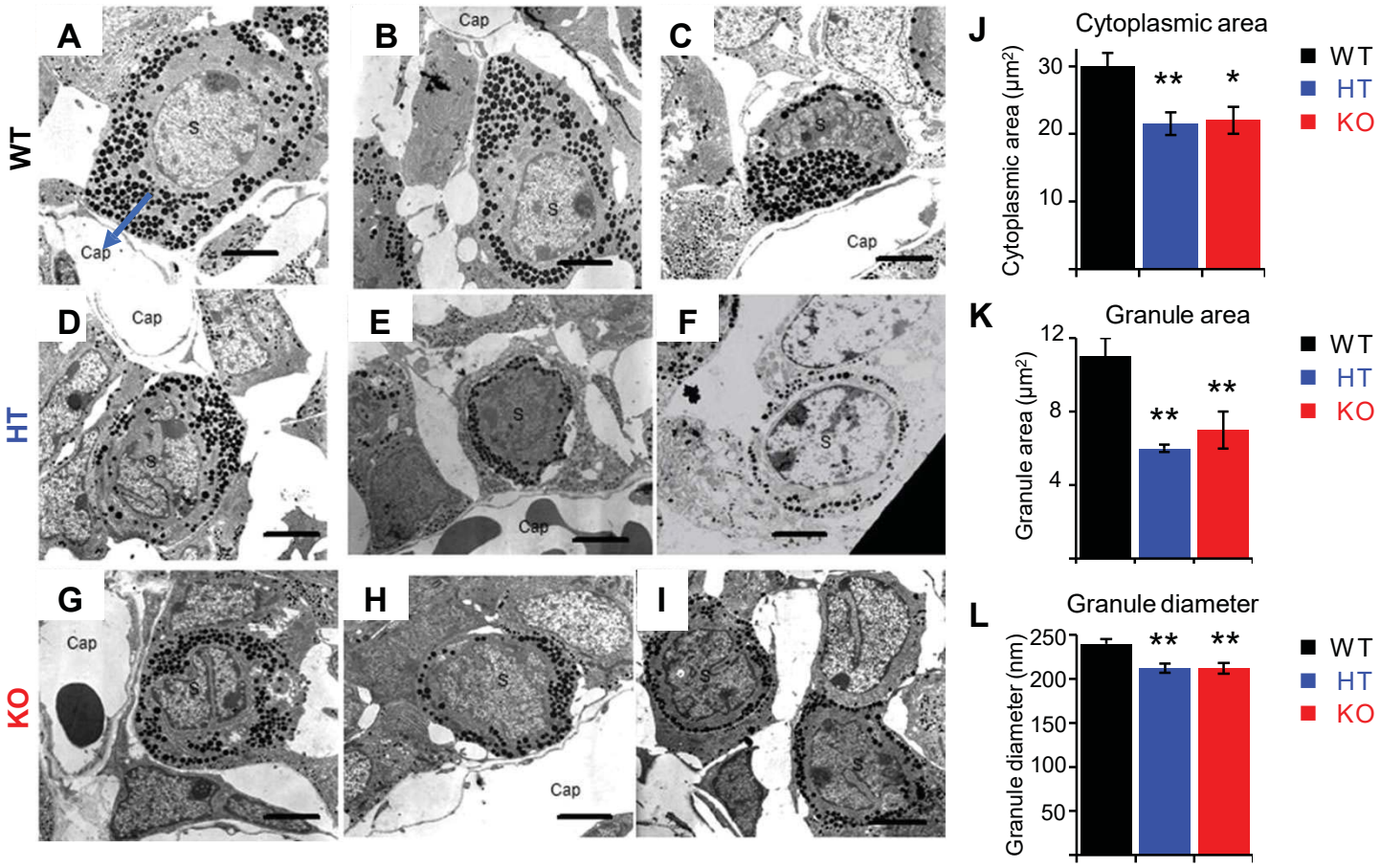
A
B
C
D
E
F
G
H
I
WT
HT
KO
Cap
S
J
Cytoplasmic area
Cytoplasmic area (μm²)
30
20
10
**
*
K
Granule area
Granule area (μm²)
12
8
4
**
**
L
Granule diameter
Granule diameter (nm)
250
200
150
100
50
**
**
WT
HT
KO

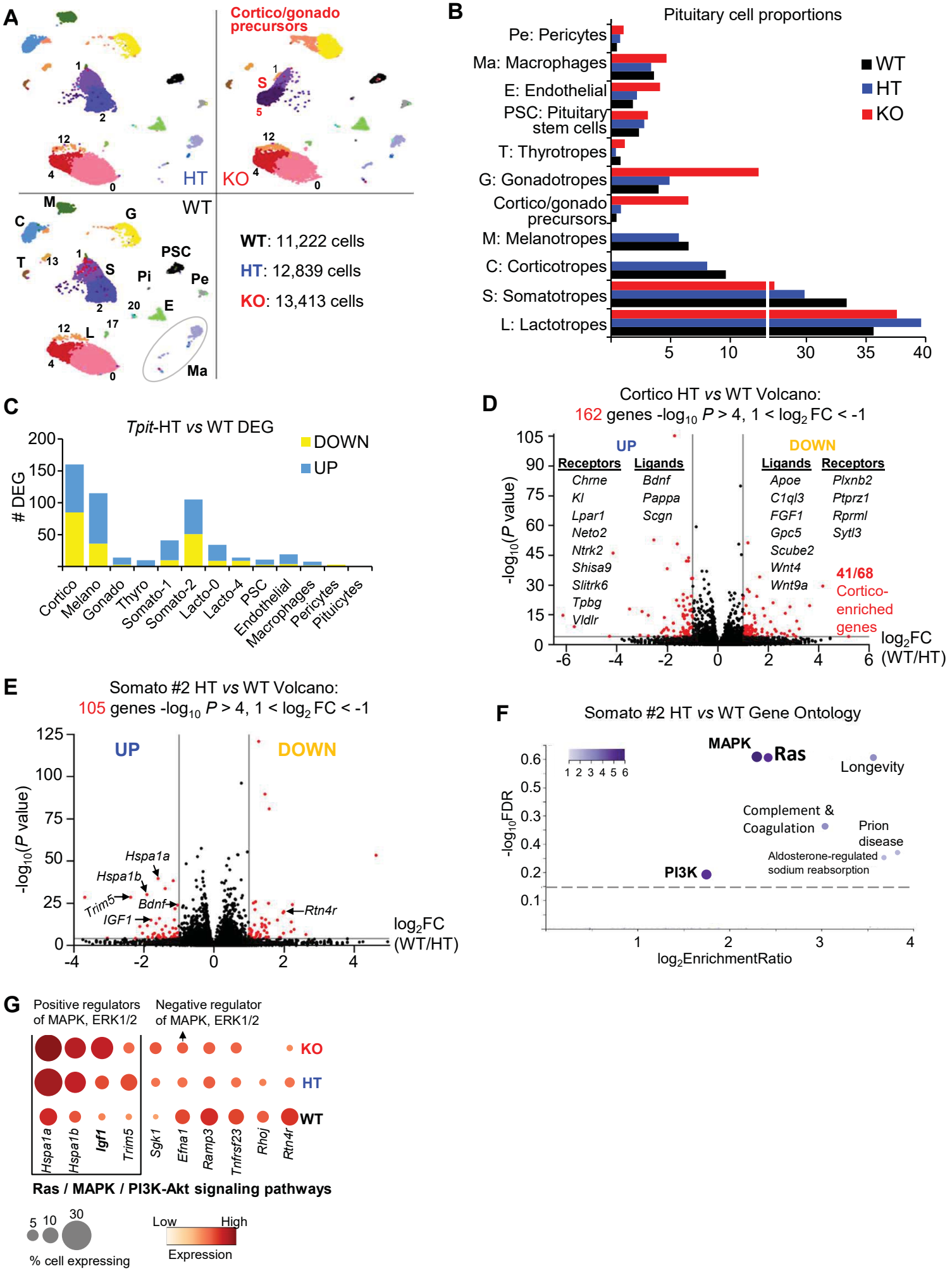
A
Cortico/gonado precursors
HT
KO
WT
WT: 11,222 cells
HT: 12,839 cells
KO: 13,413 cells
B
Pituitary cell proportions
Pe: Pericytes
Ma: Macrophages
E: Endothelial
PSC: Pituitary stem cells
T: Thyrotropes
G: Gonadotropes
Cortico/gonado precursors
M: Melanotropes
C: Corticotropes
S: Somatotropes
L: Lactotropes
WT
HT
KO
C
Tpit-HT vs WT DEG
DEG
DOWN
UP
Cortico
Melano
Gonado
Thyro
Somato-1
Somato-2
Lacto-0
Lacto-4
PSC
Endothelial
Macrophages
Pericytes
Pituicytes
D
Cortico HT vs WT Volcano:
162 genes -log10 P > 4, 1 < log2 FC < -1
UP
DOWN
Receptors
Ligands
Chrne
Kl
Lpar1
Neto2
Ntrk2
Shisa9
Slitrk6
Tpbg
Vldlr
Bdnf
Pappa
Scgn
Ligands
Receptors
Apoe
C1ql3
FGF1
Gpc5
Scube2
Wnt4
Wnt9a
Plxnb2
Ptprz1
Rprml
Sytl3
41/68
Cortico-enriched genes
-log10(P value)
log2FC (WT/HT)
E
Somato #2 HT vs WT Volcano:
105 genes -log10 P > 4, 1 < log2 FC < -1
UP
DOWN
Hspa1a
Hspa1b
Trim5
Bdnf
IGF1
Rtn4r
-log10(P value)
log2FC (WT/HT)
F
Somato #2 HT vs WT Gene Ontology
MAPK
Ras
Longevity
Complement & Coagulation
Prion disease
Aldosterone-regulated sodium reabsorption
PI3K
-log10FDR
log2EnrichmentRatio
G
Positive regulators of MAPK, ERK1/2
Negative regulator of MAPK, ERK1/2
KO
HT
WT
Hspa1a
Hspa1b
Igf1
Trim5
Sgk1
Efna1
Ramp3
Tnfrsf23
Rhoj
Rtn4r
Ras / MAPK / PI3K-Akt signaling pathways
% cell expressing
Low
High
Expression

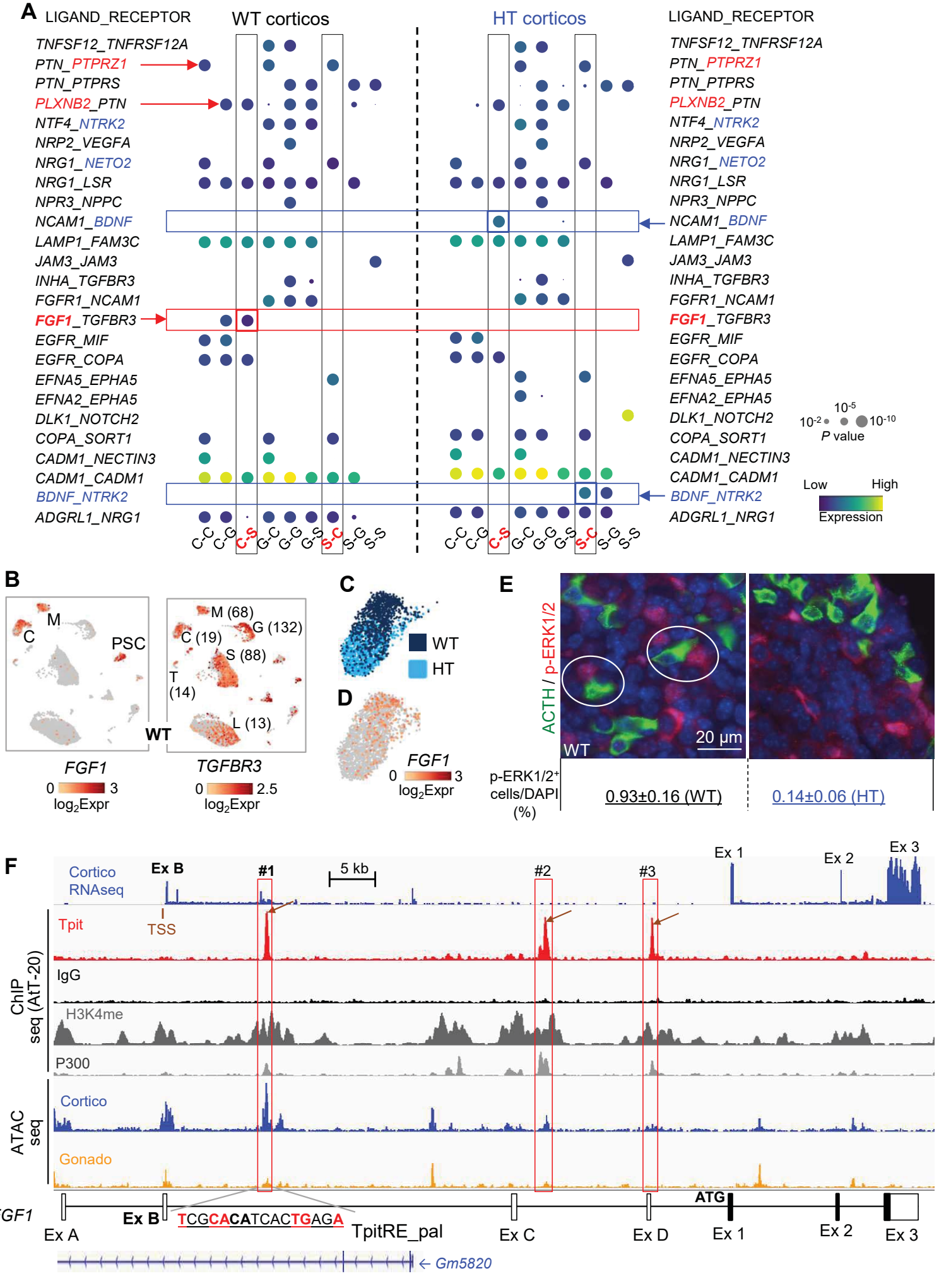
A
LIGAND_RECEPTOR
WT corticos
HT corticos
LIGAND_RECEPTOR
TNFSF12_TNFRSF12A
PTN_PTPRZ1
PTN_PTPRS
PLXNB2_PTN
NTF4_NTRK2
NRP2_VEGFA
NRG1_NETO2
NRG1_LSR
NPR3_NPPC
NCAM1_BDNF
LAMP1_FAM3C
JAM3_JAM3
INHA_TGFBR3
FGFR1_NCAM1
FGF1_TGFBR3
EGFR_MIF
EGFR_COPA
EFNA5_EPHA5
EFNA2_EPHA5
DLK1_NOTCH2
COPA_SORT1
CADM1_NECTIN3
CADM1_CADM1
BDNF_NTRK2
ADGRL1_NRG1
C-C C-G C-S G-C G-G G-S S-C S-G S-S
10-5
10-2
10-10
P value
Low
High
Expression
B
M
C
PSC
WT
M (68)
G (132)
C (19)
S (88)
T (14)
L (13)
FGF1
0 3
log2Expr
TGFBR3
0 2.5
log2Expr
C
WT
HT
D
FGF1
0 3
log2Expr
E
ACTH / p-ERK1/2
WT
20 μm
p-ERK1/2+ cells/DAPI (%)
0.93±0.16 (WT)
0.14±0.06 (HT)
F
Cortico RNAseq
Ex B
#1
5 kb
#2
#3
Ex 1
Ex 2
Ex 3
TSS
Tpit
IgG
H3K4me
P300
ChIP seq (AtT-20)
Cortico
Gonado
ATAC seq
FGF1
Ex A
Ex B
TCGCACATCACTGAGA
TpitRE_pal
Ex C
Ex D
ATG
Ex 1
Ex 2
Ex 3
← Gm5820

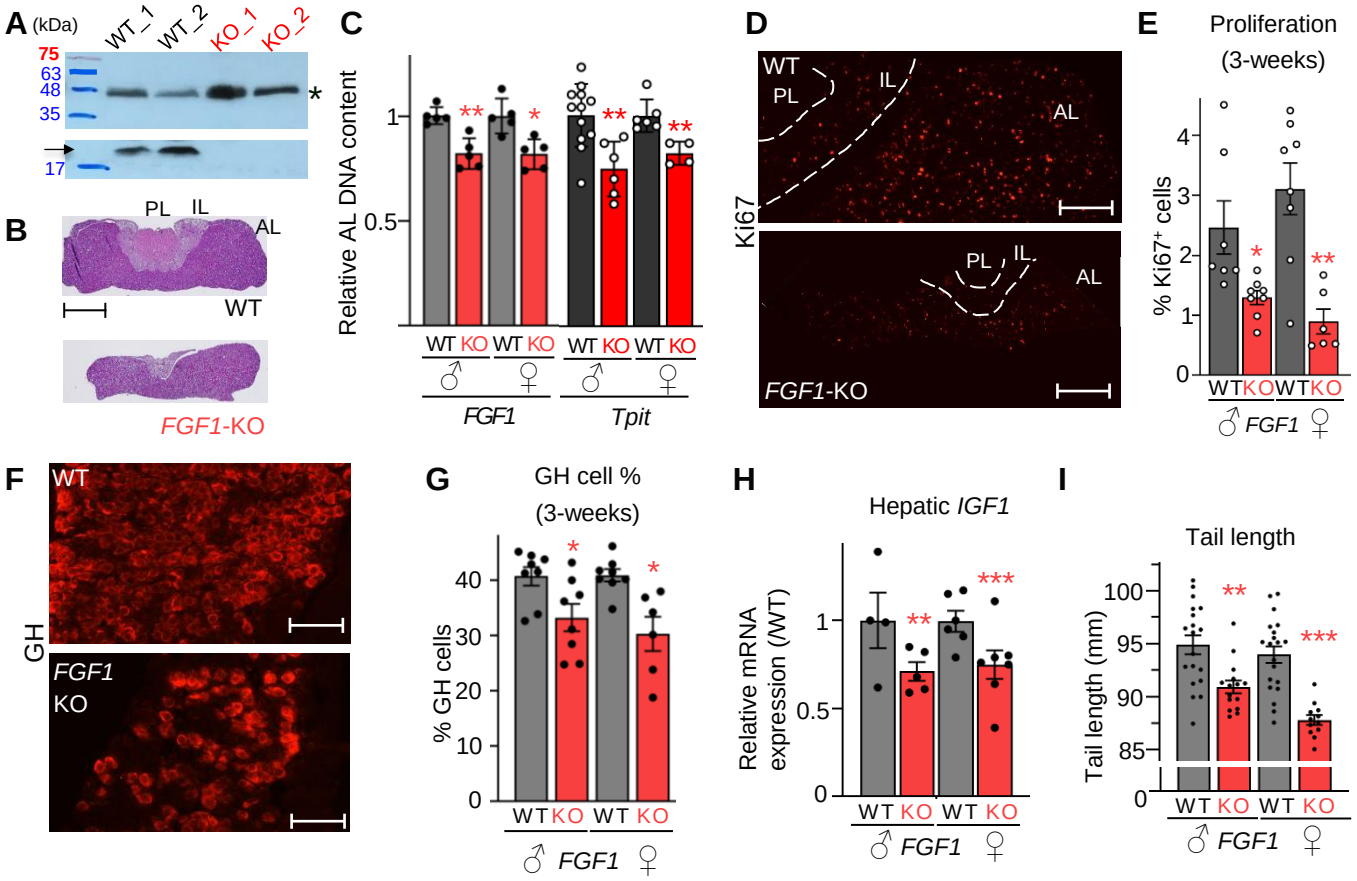
A (kDa)
WT_1
WT_2
KO_1
KO_2
75
63
48
35
17
*
B
PL
IL
AL
WT
FGF1-KO
C
Relative AL DNA content
1
0.5
**
*
**
**
WT KO WT KO WT KO WT KO
♂ ♀ ♂ ♀
FGF1
Tpit
D
WT
PL
IL
AL
Ki67
PL
IL
AL
FGF1-KO
E
Proliferation
(3-weeks)
% Ki67+ cells
4
3
2
1
0
*
**
WT KO WT KO
♂ FGF1 ♀
F
WT
GH
FGF1
KO
G
GH cell %
(3-weeks)
% GH cells
40
30
20
10
0
*
*
WT KO WT KO
♂ FGF1 ♀
H
Hepatic IGF1
Relative mRNA
expression (/WT)
1
0.5
0
**
***
WT KO WT KO
♂ FGF1 ♀
I
Tail length
Tail length (mm)
100
95
90
85
0
**
***
WT KO WT KO
♂ FGF1 ♀

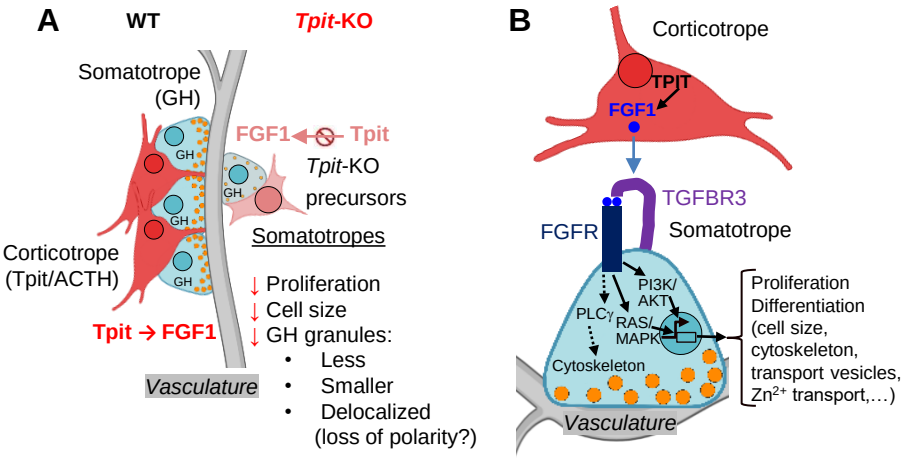
A
WT
Tpit-KO
Somatotrope
(GH)
FGF1
Tpit
Tpit-KO
precursors
GH
Somatotropes
Corticotrope
(Tpit/ACTH)
↓ Proliferation
↓ Cell size
↓ GH granules:
• Less
• Smaller
• Delocalized
(loss of polarity?)
Tpit → FGF1
Vasculature
B
Corticotrope
TPIT
FGF1
TGFBR3
FGFR
Somatotrope
PI3K/
AKT
PLCγ
RAS/
MAPK
Cytoskeleton
Proliferation
Differentiation
(cell size,
cytoskeleton,
transport vesicles,
Zn2+ transport,…)
Vasculature